




Isothermal oxidation behavior of a new Re-free nickel-based single-crystal superalloy at 950 °C

Xue-Feng Zhou, Guang Chen* , Ya-Ya Feng, Zhi-Xiang Qi, Min-Zhi Wang, Pei Li, Jia-Lin Cheng

Received: 29 May 2015 / Revised: 5 December 2015 / Accepted: 17 May 2016 / Published online: 21 June 2016
© The Nonferrous Metals Society of China and Springer-Verlag Berlin Heidelberg 2016

Abstract The isothermal oxidation behavior of a new Re-free nickel-based single-crystal superalloy in air at 950 °C for 200 h was studied by scanning electron microscopy (SEM) with energy-dispersive spectroscopy (EDS) and X-ray diffraction (XRD). The results indicate that oxidation kinetics obeys parabolic law approximately, and the mass gain increases rapidly during initial oxidation stage and then gradually slows down. The oxidation scales are composed of three layers: the outer layer mainly consists of NiO with a small amount of CoO; the intermediate layer is mainly composed of Cr₂O₃ with a small amount of spinel compounds such as CrTaO₄, NiCr₂O₄, CoCrAl₂O₄, CoAl₂O₄, and NiAl₂O₄; and the inner layer is composed of Al₂O₃. Inner Al₂O₃ layer suppresses the diffusion of elements between oxygen and alloy elements, slows down the alloy oxidation speed, and also suppresses the growth of the oxide scale and reduces the oxidation rate, which is agreeable with the oxidation kinetics.

Keywords Nickel-based single-crystal superalloy; Isothermal oxidation; Oxidation kinetic; Surface morphology

X.-F. Zhou, G. Chen*, Y.-Y. Feng, Z.-X. Qi, M.-Z. Wang, P. Li
Engineering Research Center of Materials Behavior and Design
Ministry of Education, Nanjing University of Science and
Technology, Nanjing 210094, China
e-mail: gchen@njust.edu.cn

X.-F. Zhou
School of Chemistry and Materials Engineering, Changshu
Institute of Technology, Changshu 215500, China

J.-L. Cheng
School of Materials Science and Engineering, Nanjing Institute
of Technology, Nanjing 211167, China

1 Introduction

Nickel-based single-crystal superalloys are extremely crucial selection for advanced aero-engine turbine blades due to their excellent creep and fatigue resistances [1–6]. Owing to the fact that nickel-based single-crystal superalloys are usually used at high temperature, oxidation resistance is an important property for advanced high-temperature structural material and becomes one of the integral performance indicators for evaluating a new nickel-based superalloy. To enhance oxidation resistance, more Cr and Al are added so as to generate continuous Cr₂O₃ or Al₂O₃ oxide scales at high temperature [7–11]. In addition, some studies showed that Re element can significantly enhance creep resistance and improve oxidation resistance of single-crystal superalloy [12, 13]. However, the high cost, high density, and the precipitation tendency of harmful topologically close-packed (TCP) phases restrict the addition of Re [14–19]. Therefore, it is important to design new Re-free nickel-based superalloys [20–22] and investigate the high-temperature oxidation behavior, which is close to the superalloy compositions. The high oxidation resistance can be evaluated by studies of isothermal oxidation behaviors for nickel-based single-crystal superalloys through analyzing oxidation kinetics and oxidation products [23–26].

The present work reported a new Re-free nickel-based single-crystal superalloy which is comparable to the second-generation Re-containing nickel-based single-crystal superalloy from GE Company [27, 28]. Microstructures and mechanical properties of the new Re-free nickel-based single-crystal superalloy were characterized in previous report [28]. The isothermal oxidation kinetic, oxidation products, surface morphology, and scale formation mechanism at 950 °C were also investigated to evaluate the high

oxidation resistance in this work. It is badly in need of decreasing the manufacturing cost and significantly promoting the commercial applications of new Re-free superalloys.

2 Experimental

The compositions of new Re-free superalloy were 7.500 wt% Cr, 5.000 wt% Co, 2.000 wt% Mo, 6.100 wt% Al, 8.000 wt% W, 6.500 wt% Ta, 0.150 wt% Hf, 0.050 wt% C, 0.004 wt% B, 0.015 wt% Y, and balance Ni. The single-crystal rods with a diameter of 8 mm and a length of 100 mm were prepared by seeded method using a vacuum induction directional solidification technology with withdraw velocities of $50 \mu\text{m}\cdot\text{s}^{-1}$, at the holding temperature of 1823 K, and the detail experiments were shown elsewhere [28]. And then, the single-crystal rods were heat-treated by 1300 °C/3 h/AC + 1100 °C/4 h/AC + 870 °C/24 h/AC (AC: air cooling) and cut into a diameter of 6 mm and a length of 10 mm perpendicular to the growth direction. The specimens were placed into Al_2O_3 crucibles and heated in an electrical resistance furnace. The weight of specimens was measured by an electronic balance with a resolution of 0.1 mg after cooling to room temperature. The oxidation kinetics was studied by means of discontinuous thermogravimetric (including flaking oxides) analysis. Scanning electron microscopy (SEM) with energy-dispersive spectroscopy (EDS) and X-ray diffraction (XRD) (using $\text{Cu K}\alpha$ radiation and the penetrating ability reaching $\sim 10 \mu\text{m}$) were used to characterize the morphology, composition, and phase structure of oxide scale of the single-crystal superalloy, respectively.

3 Results and discussion

3.1 Oxidation kinetics

The isothermal oxidation curve of the superalloy at 950 °C for 200-h oxidation is shown in Fig. 1. It can be seen that the mass gain increases rapidly during the initial oxidation stage, and then, the mass change gradually slows down and keeps a relative smooth stage.

The oxidation kinetics of the superalloy approximately agrees with parabolic law after oxidation at 950 °C for 200 h. At initial oxidation stage, the standard free energy of all kinds of oxides is negative, and the oxidation process of the alloy is mainly controlled by the formation and growth of NiO with a small amount of CoO, resulting in a quick mass change. With the exposure time increasing, the diffusion of elements in the oxide scale dominates the growth of oxide scale and stable Al_2O_3 is generated. This

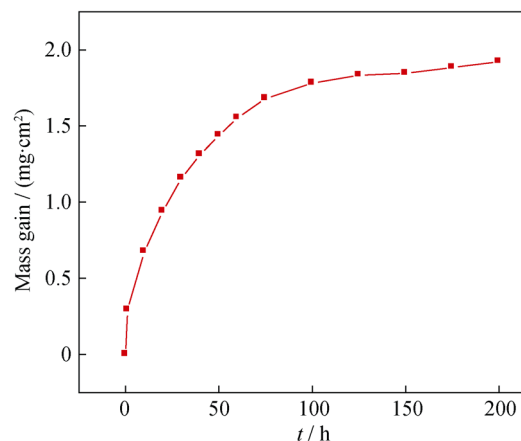


Fig. 1 Oxidizing curve of superalloy at 950 °C

oxidation process is controlled by the formation and growth of Al_2O_3 , and the mass changes slowly on the performance of the oxidation kinetic. After 40-h oxidation, the oxide scale is sufficiently thick to suppress the diffusion of alloying elements and the growth of the oxide scale, thus the oxidation of the alloy achieves a relatively stable stage. However, as the oxidation prolongs, some oxides would flake or volatilize, resulting in internal oxidation or nitridation of alloying elements, eventually leading to that the oxidation kinetics slightly deviates from the parabolic law.

3.2 Surface morphologies and XRD analysis

Figure 2 shows the morphologies of the superalloys after oxidation for 1, 100, and 200 h. As shown, the oxides are uniformly distributed on the alloy surface, and with the exposure time increasing, the crystalline size of oxidation scale increases significantly. No obvious spallation of the oxide films is detected in the sample after 100-h oxidation, but some spallations are clearly shown on the surface of the superalloy after 200-h oxidation. The oxidation products are mainly composed of NiO with a small amount of CoO for the superalloy after 1-h oxidation, as shown in Fig. 3. When the oxidation time increases to 100 h, a large number of Al_2O_3 and a small amount of Cr_2O_3 are formed, accompanying with generating some spinel oxides such as CrTaO_4 , NiCr_2O_4 , CoCr_2O_4 , NiAl_2O_4 , and CoAl_2O_4 . For the sample with 200-h oxidation, the amount of Al_2O_3 continues to increase but that of CrTaO_4 decreases.

The high-temperature oxidation behavior of nickel-based single-crystal superalloy depends on the alloy composition. By addition of a certain amount of Al or Cr, which induces the formation of a protective oxide scale of Cr_2O_3 or Al_2O_3 , the oxidation resistance of the superalloy can be improved. At initial oxidation stage, oxygen is absorbed rapidly on the alloy surface, and various oxides such as Al_2O_3 , NiO, CoO, and Cr_2O_3 are formed by the

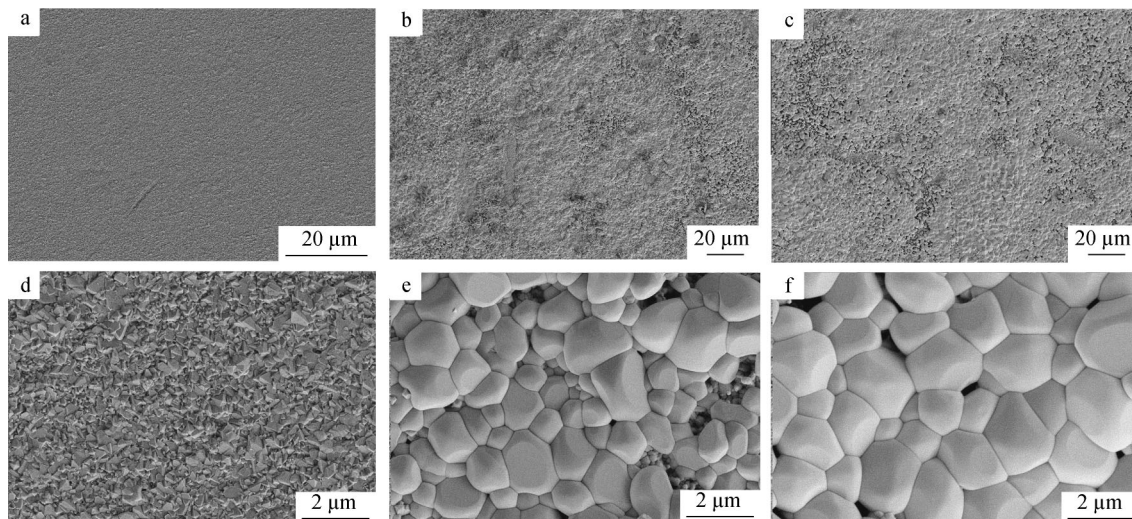


Fig. 2 SEM images of scale morphologies of superalloy oxidized for **a, d** 1 h, **b, e** 100 h and **c, f** 200 h at 950 °C

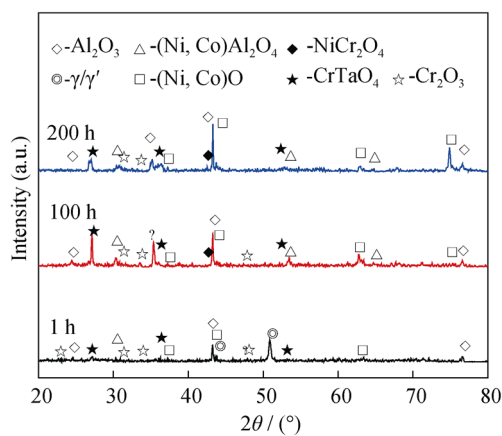


Fig. 3 Oxide phases detected by XRD after oxidation at 950 °C for different time

reaction with the alloy elements. With the oxidation time increasing, NiO scale grows relatively fast and a single cover layer of NiO is formed on the surface of the alloy. As the oxidation time prolongs, Cr₂O₃ and Al₂O₃ are formed by reacting selectively between oxygen and matrix elements when oxygen diffuses through the NiO layer. Then, the diffusion of Ni would be inhibited when the content of Al or Cr exceeds the critical value that would form a continuous Al₂O₃ or Cr₂O₃ oxide scale, and NiO growth would be inhibited. Meanwhile, the spinels are formed by two ways. The first way is by solid-state reaction of oxides with nickel and dissolved oxygen in the scale according to: Cr₂O₃ + Ni + 1/2O₂ → NiCr₂O₄, Al₂O₃ + Ni + 1/2O₂ → NiAl₂O₄ and 4NiO + 2Ta₂O₅ + O₂ → 4NiTaO₄. The second one is by oxide–oxide reaction to form spinels according to Cr₂O₃ + NiO → NiCr₂O₄ and Al₂O₃ + NiO → NiAl₂O₄ [29].

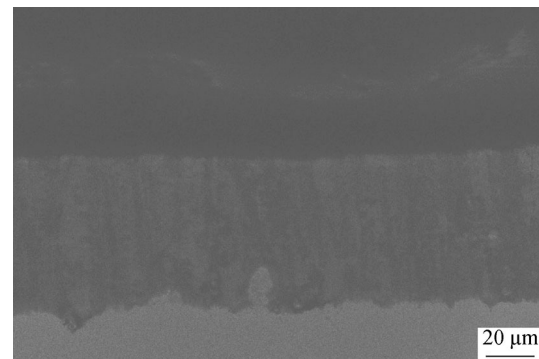


Fig. 4 Cross-sectional BSE image of superalloy after oxidation at 950 °C for 200 h

3.3 Cross-sectional morphology

The cross-sectional backscattered electron (BSE) image of the superalloy after 200-h oxidation at 950 °C is shown in Fig. 4, and the oxide scale has a distinct, continuous, and dense layer structure. Figure 5 shows elemental distributions. Ni, Co, and O are mainly concentrated in the outer layer; Cr, Ni, Ta, and W are concentrated in the intermediate layer; and Al and O significantly are enriched in the inner layer. According to the results of XRD, it can be proposed that the outer, intermediate, and inner layers consist of NiO layer, complex spinels such as CrTaO₄, NiCr₂O₄, CoCrAl₂O₄, CoAl₂O₄, NiAl₂O₄, and Al₂O₃ layer, respectively.

The cross-sectional oxidation scale is relatively uniform, and only some minor voids appear in the subsurface. This is due to the different volume expansion produced by the formation of Al₂O₃ and Cr₂O₃, which makes the oxide scale and the substrate in a high stress state and results in

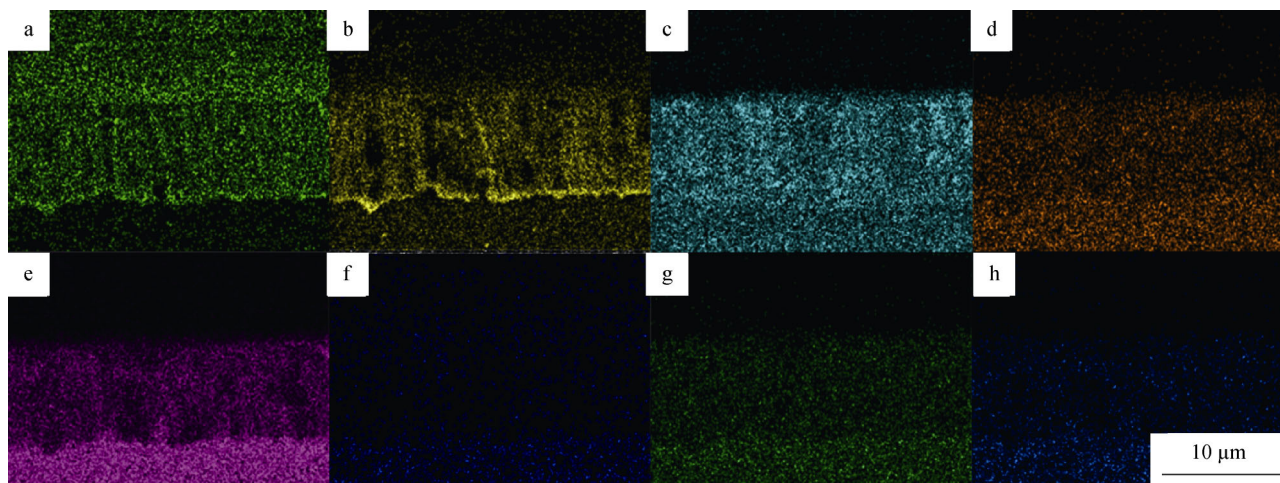


Fig. 5 Elemental distributions of cross section after oxidation at 950 °C for 200 h in air: **a** O, **b** Al, **c** Cr, **d** Co, **e** Ni, **f** Mo, **g** Ta, and **h** W

the oxides crack or even falling off, thus providing a diffusion channel for O [29, 30]. Elements in the matrix continue to diffuse toward outer driving by the different concentrations, and the matrix will be oxidized to form Al_2O_3 , Cr_2O_3 , and other oxides when they meet O. Meanwhile, some Cr_2O_3 peels off due to the formation of NiAl_2O_4 by the reaction of Al_2O_3 and NiO, leading to the formation of an incompletely continuous and dense internal Al_2O_3 scale. Oxygen in the air diffuses into the matrix along the minor voids of the outer oxide layer, and an internal Al_2O_3 scale is formed by the reaction between Al and O, which lowers oxygen diffusion into the matrix. Also, the formation of spinels scale decreases the oxygen activity between the matrix and the scale, but the selective oxidation of Al may still occur in spite of low concentration of Al in the alloy, leading to that Al is enriched in the interface between the outer oxide layer and the substrate and a straight and continuous intermediate Al_2O_3 layer is formed. Inner Al_2O_3 layer suppresses the relative diffusion between oxygen and alloy elements, slows down the alloy oxidation speed, and also suppresses the growth of the oxide scale and reduces the oxidation rate, which is agreeable with the oxidation kinetic.

4 Conclusion

The oxidation mechanism in air of the new Re-free nickel-based single-crystal superalloy was determined by both oxidation kinetic and XRD–SEM studies. The oxidation kinetics of the superalloy at 950 °C for 200 h obeys the parabolic law, which is controlled by the formation of NiO in initial oxidation stage, and then the element diffusion depends on the growth and replacement of oxide scale with exposure time increasing. The oxide scales consist of three

layers: the outer layer mainly consisting of NiO with a small amount of CoO; the intermediate layer mainly consisting of Cr_2O_3 with a small amount of spinel compounds such as CrTaO_4 , NiCr_2O_4 , $\text{CoCrAl}_2\text{O}_4$, CoAl_2O_4 , and NiAl_2O_4 ; and the inner layer consisting of Al_2O_3 . Inner Al_2O_3 layer suppresses the diffusion of elements between oxygen and alloy elements, slows down the alloy oxidation speed, and also suppresses the growth of the oxide scale and reduces the oxidation rate.

Acknowledgments This study was financially supported by Jiangsu Province Key Technology R&D (Industry) Program (No. BE201217), the Science and Technology Innovation Fund Program (Nos. CX2011028 and CX2011029), the Cooperative Innovation Fund of Jiangsu Province (No. BY2014004-09), and the Foundation of Jiangsu Key Laboratory of Advanced Structural Materials and Application Technology (No. ASMA201403).

References

- [1] Duhl MGDN, Giamei AF. The development of single crystal superalloy turbine blades. In: *Superalloys*. Warrendale; 1980. 41
- [2] McLean M, Webster GA, Nabarro FRN, Cottrell A. Nickel-base superalloys: current status and potential. *Philos Trans R Soc London Ser A Phys Eng Sci*. 1995;351(1697):419.
- [3] Pineau A, Antolovich SD. High temperature fatigue of nickel-base superalloys—a review with special emphasis on deformation modes and oxidation. *Eng Fail Anal*. 2009;16(8):2668.
- [4] Celed AD, Duhl DN. Second-generation nickel-base single crystal superalloy. In: *Superalloys*. Warrendale; 1988. 235.
- [5] Hashizume R, Yoshinari A, Kiyono T, Murata Y, Morinaga, M. Development of Ni-based single crystal superalloys for power-generation gas turbines. In: *Superalloys*. Warrendale; 2004. 483.
- [6] Koizumi Y, Kobayashi T, Yokokawa T, Zhang J X, Osawa M, Harada H, Aoki Y, Arai M. Development of next-generation Ni-base single crystal superalloys. In: *Superalloys*. Warrendale; 2004. 35.

- [7] Wakasa K, Yamaki M. High-temperature oxidation behaviour of base metal elements in nickel-base alloys. *J Mater Sci*. 1988; 23(4):1459.
- [8] Barnard BR, Liaw PK, Buchanan RA, Klarstrom DL. Affects of applied stresses on the isothermal and cyclic high-temperature oxidation behavior of superalloys. *Mater Sci Eng A*. 2010; 527(16):3813.
- [9] Han S, Young DJ. Simultaneous internal oxidation and nitridation of Ni–Cr–Al alloys. *Oxid Metals*. 2001;55(3–4):223.
- [10] Chen JH, Rogers PM, Little JA. Oxidation behavior of several chromia-forming commercial nickel-base superalloys. *Oxid Metals*. 1997;47(5–6):381.
- [11] Kofstad P. Defects and transport properties of metal oxides. *Oxid Metals*. 1995;44(1–2):3.
- [12] Reed RC, Tao T, Warnken N. Alloys-by-design: application to nickel-based single crystal superalloys. *Acta Mater*. 2009; 57(19):5898.
- [13] Caron P, Khan T. Evolution of Ni-based superalloys for single crystal gas turbine blade applications. *Aerosp Sci Technol*. 1999;3(8):513.
- [14] Liu CT, Sun XF, Guan HR, Hu ZQ. Oxidation of the single-crystal Ni-base superalloy DD32 containing rhenium in air at 900 and 1000 °C. *Surf Coat Technol*. 2005;197(1):39.
- [15] Seiser B, Drautz R, Pettifor DG. TCP phase predictions in Ni-based superalloys: structure maps revisited. *Acta Mater*. 2011;59(2):749.
- [16] Rae CMF, Reed RC. The precipitation of topologically close-packed phases in rhenium-containing superalloys. *Acta Mater*. 2001;49(19):4113.
- [17] Rae CMF, Karunaratne MSA, Small CJ, Broomfield RW, Jones CN, Reed RC. Topologically close packed phases in an experimental rhenium-containing single crystal superalloy. In: *Superalloys*. Warrendale; 2000. 767.
- [18] Pollock TM, Tin S. Nickel-based superalloys for advanced turbine engines: chemistry, microstructure and properties. *J Propuls Power*. 2006;22(2):361.
- [19] Tin S, Pollock TM. Phase instabilities and carbon additions in single-crystal nickel-base superalloys. *Mater Sci Eng A*. 2003; 348(1):111.
- [20] Sato A, Harada H, Yokokawa T, Murakumo T. The effects of ruthenium on the phase stability of fourth generation Ni-base single crystal superalloys. *Scr Mater*. 2006;54(9):1679.
- [21] Morinaga M, Yukawa N, Adachi H, Ezaki H. New PHACOMP and its application to alloy design. In: *Superalloys*. Warrendale; 1984. 523.
- [22] Murata Y, Miyazaki S, Morinaga M, Hashizume R. Hot corrosion resistant and high-strength nickel-based single crystal and directionally-solidified superalloys developed by the d-electrons concept. In: *Superalloys*. Warrendale; 1996. 61.
- [23] Zhang JS, Hu ZQ, Murata Y, Morinaga M, Yukawa N. Design and development of hot corrosion-resistant nickel-base single-crystal superalloys by the d-electrons alloy design theory: part II. Effects of refractory metals Ti, Ta, and Nb on microstructures and properties. *Mater Trans*. 1993;24(11):2451.
- [24] Li MH, Sun XF, Li JG, Zhang ZY, Jin T, Guan HR, Hu Z. Oxidation behavior of a single-crystal Ni-base superalloy in air. I: at 800 and 900 °C. *Oxid Metals*. 2003;59(5–6):591.
- [25] Li MH, Sun XF, Guan HR, Hu ZQ. Oxidation behavior of a single crystal Ni-base superalloy in air. II: at 1000, 1100, and 1150 °C. *Oxid Metals*. 2003;60(1–2):195.
- [26] Göbel M, Rahmel A, Schütze M. The isothermal-oxidation behavior of several nickel-base single-crystal superalloys with and without coatings. *Oxid Metals*. 1993;39(3–4):231.
- [27] Cincinnati CSW, Loveland LBJ. Property-balanced nickel-base superalloys for producing single crystal articles. US Patent; 6074602. 2000.
- [28] Zhou XF, Chen G, Yan ST, Zheng G, Li P, Chen F. Exploration and research of a new Re-free nickel-based single crystal superalloy. *Acta Metall Sin*. 2013;49(11):1467.
- [29] Christ HJ, Chang SY, Krupp U. Thermodynamic characteristics and numerical modeling of internal nitridation of nickel base alloys. *Mater Corros*. 2003;54(11):887.
- [30] Litz J, Rahmel A, Scharr M. Selective carbide oxidation and internal nitridation of the Ni-base superalloys IN 738 LC and IN 939 in air. *Oxid Metals*. 1988;30(1–2):95.